Correction of the Jitter Effect in Pléiades Satellite Elevation Data for Enhanced 3D Change Monitoring

Imen Brini, Denis Feurer, Riadh Tebourbi, Fabrice Vinatier, Riadh Abdelfattah

Correction of the Jitter Effect in Pléiades Satellite Elevation Data for Enhanced 3D Change Monitoring

Imen Brini[1,2], Denis Feurer[1], Riadh Tebourbi[2], Fabrice Vinatier[1], and Riadh Abdelfattah[2]

[1] UMR LISAH, Univ. Montpellier, AgroParisTech, INRAE, IRD, Institut Agro Montpellier, Montpellier, France
[2] Higher School of Communications of Tunis COSIM Lab, University of Carthage, Tunis, Tunisia
imen.brini@ird.fr

Abstract. The satellite jitter effect observable in the digital elevation model of difference, herein referred to as DoD, generated using tri-stereo pairs of Pléiades images is a common phenomenon that can reduce the precision of elevation measurements making it challenging for 3D change detection in the land surface. To address this issue, previous studies used correction methods based on polynomial and sinusoid fitting to reduce the jitter effect. However, such approaches do not entirely remove these undulations. In this paper, the image noise reduction task is framed as a signal filtering problem, to eliminate these repetitive patterns while preserving relevant information for accurate change detection using Fourier transform. The noise frequency is identified through the frequency spectrum using a threshold-based method, allowing the subsequent application of a finite impulse response filter to remove the noise. Experiments conducted on Pléiades DoDs data covering the Lebna watershed located in the north of Tunisia validate the effectiveness of this approach. The results demonstrate that the Fourier transform-based filtering method significantly outperforms the state-of-the-art methods, both in terms of qualitative visual assessment and quantitative performance metrics.

Keywords: Satellite jitter · Fourier transform · DEM of difference · 3D change

1 Introduction

Multi-temporal surface elevation data are derived from recurrent data acquisitions that are captured with various sensors, and processed using different 3D reconstruction approaches adapted for the selected sensor. The differencing between these datasets is a simple approach to examine potential changes. Recently, optical satellite systems have been able to provide very high-resolution products with minimal errors.

In order to compare two multi-temporal datasets, it is required to ensure a precise spatial co-registration, such that the pixels of each dataset represent the

same location in the Earth surface. Insufficient spatial fit causes uncertainties that lead to the identification of artifact changes. Apart from miss-registration, biases have also been related to the satellite acquisition geometry, especially the attitude parameters, which can be significant enough to necessitate correction. For instance, the variation in the satellite's attitude, known as satellite jitter, introduces biases within the captured images and their derivatives (e.g. Digital Elevation Models (DEMs), and DEM of difference (DoD)). Consequently, the corrections are only applied to the data products where the jitter is observable [8].

Satellite jitter is a source of random errors originating from the periodic motion of the dynamic structure on board, the temperature change resulting from orbital changes, along with other factors [12]. Consequently, in the push-broom imaging process of the optical satellite, there are different deviations between adjacent imaging lines, reducing the radiometric and geometric quality of the image [11].

Previous studies highlighted the effect of jitter and reported its influence on optical satellites. The frequency and amplitude of the jitter from the Terra satellite are about 1.5 Hz and 0.2–0.3 pixels, respectively, corresponding to 6-9 m on the ground [10]. The non-modeled jitter of the QuickBird satellite induces nearly 5 pixels corresponding to 2.5 m geometric distortion with a frequency of 1 Hz, and 0.2 pixel corresponding to 0.1 m geometric distortion with a frequency of 4.3 Hz [1]. Shean et al. [9] linked the along-track elevation errors with magnitude of $\sim$ 0.1–0.5 m to the non-modeled jitter effect of the WorldView satellite.

It is challenging to detect the jitter effect from each DEM due to its relatively low amplitude compared to the terrain variation in most scenarios. In contrast, deriving the DoD, for change detection purposes, significantly eliminates the topography signal and reflects the superposition of the jitter effects from both DEMs along with terrain change [7].

In attempts to correct the jitter effect, Nuth and Kääb [8] fitted high order polynomials (6th to 8th order) to the elevation differences with across- and along-track biases to adjust one of the DEMs. Girod et al. [7] fit a polynomial on the across-track direction. The order of the polynomial is determined by iterative fitting until there is no further noticeable improvement in the root mean square error. For the along-track direction, two sums of sines are iteratively fit to remove a first long jitter wavelength ($\sim$ 34 km) with a large amplitude ($\pm$10–15 m) and a second shorter jitter wavelength (4.5$\pm$0.3 km) with lower amplitude (5$\pm$5 m).

Berthier et al. [3] found that low-frequency undulating due to the jitter of the Pléiades satellite in the along-track direction has an amplitude of 1-2 m and a wavelength of approximately 4 km. Both, across- and along-track biases were corrected by fitting a fifth order polynomial and a spline respectively.

Deschamps-Berger et al. [5] pointed out the appearance of low-frequency undulation in the height of snowpack residual map. This residual map is derived from the difference between Pléiades DEM and NASA Airborne Snow Observatory airborne laser scanning DEM. The low-frequency undulation has an amplitude of 0.30 m and a wavelength of about 4 km. An empirical correction was

applied to eliminate the undulation pattern from the residual map by removing the frequencies lower than $4 \times 10^{-4}\ m^{-1}$ corresponding to a wavelength longer than 2.5 km. In the same context, Beraud et al. [2] estimated along-track undulations on Pléiades DEMs with an amplitude reaching a few decimeters and used the Fourier transform to reduce undulations higher than 1.5 km of wavelength.

The increased jitter effect in Pléiades-1B since 2021 [3] is a significant concern that impacts satellite elevation data. To further illustrate the jitter effect, a comparison between a DoD generated using Pléiades-1A and a DoD derived from Pléiades-1B could be insightful (Fig. 1). This comparison would visually highlight the differences and emphasize the need of effective corrections, enabling Pléiades-1B to perform similarly to Pléiades-1A in change detection applications.

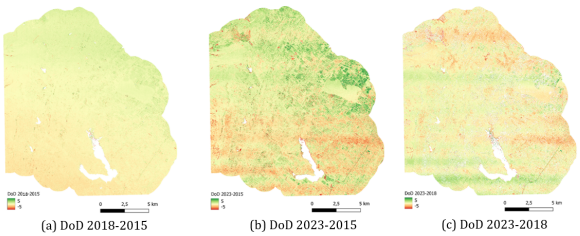

Fig. 1. (a) DoD_{18-15}, (b) DoD_{23-15}, and (c) DoD_{23-15}. Contains information © CNES (2015, 2018, 2023), Distribution Airbus DS, all rights reserved. Commercial use prohibited.

Accordingly, the filtering can be performed in the spatial domain or in the frequency domain using transformation tools, e.g., Fourier transform. The spatial domain filtering directly changes the pixels value of the image, while the frequency domain filtering modifies the frequency composition of the image. However, Berthier et al. [3] stated that using spatial filtering does not completely remove the along-track undulations.

To reduce the significance level required for detecting 3D elevation changes, it is essential to mitigate the impact of satellite jitter to restore the most relevant information.

This paper is structured as follows: section 2 describes the proposed filtering approach in the frequency domain; section 3 describes the filtering results on Pléiades DoDs; and finally, the conclusion is in section 4.

2 Methodology

2.1 Data

The Pléiades satellite system comprises two satellites Pléiades-1A and Pléiades-1B, that were launched in December 2011 and December 2012, respectively. The

satellites provide a daily revisit as they are operating in the same orbit with 180 degree offset. The sensors are able to acquire a panchromatic band with 0.7 m ground sampling distance (GSD) at the nadir and four multi-spectral bands (blue, green, red, and near-infrared) with 2.8 m GSD. Images of the Pléiades sensor are provided as a bundle of a panchromatic band upsampled to 0.5 m GSD and multi-spectral bands at 2.0 m GSD. The swath width of Pléiades image data is 20 km on ground. The Pléiades images are supplied with the rational polynomial coefficient model, which are a standard product delivered by satellite data vendors. The RPC is a projection function, that relates the image to the object space.

The particular interest in using Pléiades images to derive DEMs arises from the sensor ability to acquire tri-stereo panchromatic images in one single flight with a high spatial resolution. Furthermore, several studies have demonstrated the feasibility of generating highly accurate DEMs usig Pléiades tri-stereo images [5, 2, 3].

For this study, tri-stereo Pléiades images were ordered in 2015, 2018, and 2023 covering the Lebna watershed, located in the coastal plain in northeastern Tunisia, in the Cap Bon peninsula, through the DINAMIS platform. The images ordered in 2015 and 2018 were captured with Pléiades-1A, while the images ordered in 2023 were captured with Pléiades-1B. The panchromatic images, with a 0.5 m resolution, are used for the DEMs and DoDs generation. The DEMs were derived based on a structure-from-motion coupled with a multi-view-stereo photogrammetric workflow using the semi-global matching algorithm for dense point cloud generation. The DEMs were co-registered using the Time-SIFT approach [6, 4]. The change detection is consequently performed by DEM differencing.

2.2 Modeling approach

Biases related to the data acquisition geometry in the along-track direction are modeled from the elevation difference maps and reduced using the frequency domain approach.

In order to design the filter for noise reduction, it is essential to initially estimate its frequency. The Fourier transform of the image provides insight into the frequencies, allowing the identification of peaks that correspond to the noise. Fast Fourier transform (FFT) is an exact fast algorithm to compute the discrete Fourier transform when data are acquired on a regular grid. However, in certain image processing fields, the frequency locations are irregularly distributed, which obstructs the use of FFT.

To override the no-data values caused by sparse or missing information, a one-dimensional signal is extracted by averaging pixel values per line to estimate vertical frequency content in the along-track direction. The FFT is then applied to this signal, following this equation:

$$F_k = \sum_{n=0}^{N-1} x_n e^{\frac{-2\pi i}{N} kn} \tag{1}$$

where F is the discrete FFT of the signal, k is the frequency bin index, and N is the number of samples in the signal.

It is worth mentioning that the low frequencies should not be confused with the periodic noise caused by the jitter effect. Consequently, a threshold is predefined to maintain the lowest frequencies. This threshold corresponds to the inverse of the mean noise periodicity, ensuring that only relevant low-frequency information is retained. The most dominant frequency within the thresholded amplitude spectrum represents the specific frequency associated with the jitter noise.

Once this frequency is identified, a finite impulse response (FIR) filter is designed to reduce this frequency component while preserving the details of the image, following this equation:

$$y_n = \sum_{k=0}^{M-1} h_k x_{n-k} \tag{2}$$

where y_n is the output signal at index n, x_n is the input signal at index n, h_k are the filter coefficients, M is the filter order, and k is the index of summation over the impulse response.

This filter effectively attenuates low-frequency components while allowing higher frequencies to pass through. The convolution operation integrates the filter across each row of the image, removing the low-frequency components that correspond to the jitter, and restoring back the image in the spatial domain.

Figure 2 represents an example showing the proposed approach to identify the jitter frequency and filter it.

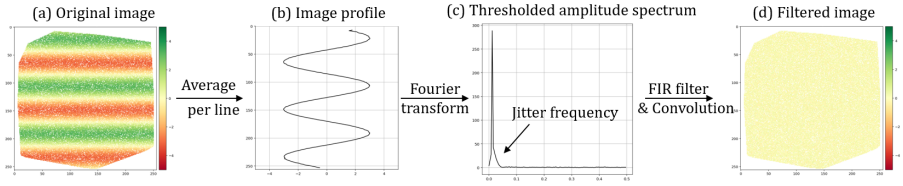

Fig. 2. Different stages of the proposed approach: (a) original image, (b) image profile (c) thresholded amplitude spectrum, and (d) filtered image. The image in (a) was generated to represent the jitter effect. The white pixels indicate no-data.

2.3 Quantitative evaluation metrics

Stable terrain is an indicator of the quality of the corrections. In the DoD, relatively flat and stable areas, that mainly correspond to road surfaces, are not expected to experience 3D changes, and their elevation difference is supposed to approach zero. Hundreds of points have been manually selected through the

study area and used for the accuracy assessment. These points values are extracted before and after filtering and evaluated in terms of mean and standard deviation and normalized median absolute deviation (NMAD). The performance of our proposed approach is compared with spatial filtering using the sum of sinusoids fit used by Girod et al. [7] and the spline fit used by Berthier et al. [3].

3 Experimental results and discussion

The DoD covering the period between 2015 and 2023 , herein reffered as DoD_{23-15}, and the DoD covering the period between 2018 and 2023, herein referred to as DoD_{23-18}, reveals an along-track jitter effect with an amplitude reaching on average 2 m and 1.5 m, respectively, and an undulation wavelength of about 2 km (Fig. 3).

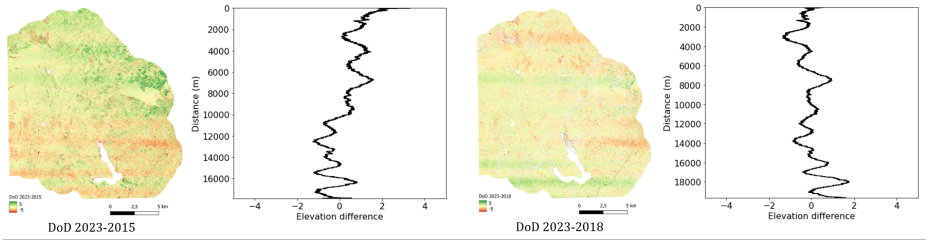

Fig. 3. DoD_{23-15} and DoD_{23-18} with their average per line, respectively. Contains information © CNES (2015, 2018), Distribution Airbus DS, all rights reserved. Commercial use prohibited.

For both DoDs, the threshold is 5×10^{-4} cycles per pixel, and accordingly the frequency for DoD_{23-15} and DoD_{23-18} is 6.8×10^{-4} cycles per pixel and 5.9×10^{-4} cycles per pixel, respectively. Table 1 shows the parameters of the compared methods.

Table 1. The parameters of the compared approaches.

Approach	Parameter	Value
Sum of sinusoid fit	Number of sinusoids	up to 6 sines
Spline fit	Smoothness parameter	50
	Threshold	5×10^{-4}
Proposed approach	Frequency	$\sim 0.6 \times 10^{-4}$
	Filter order (M)	1001

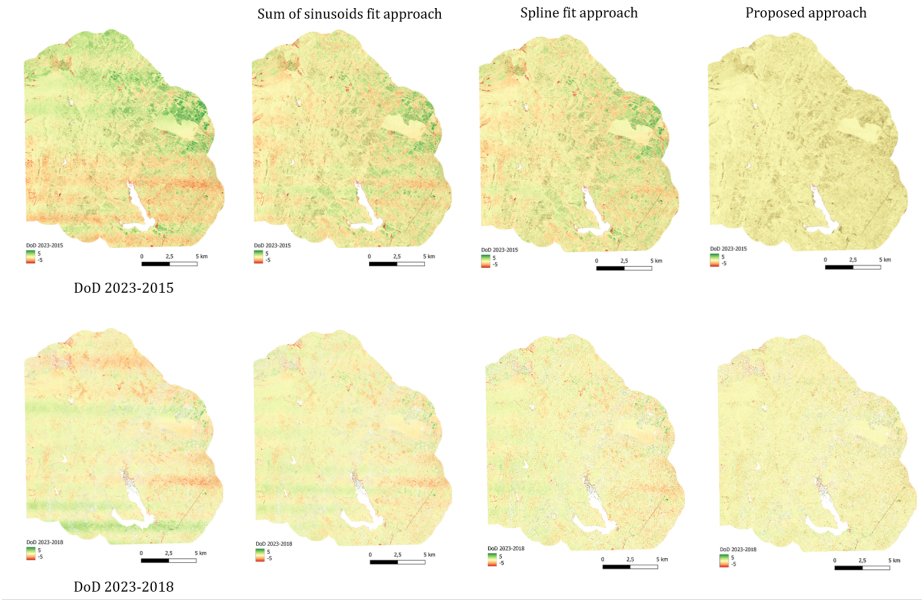

Fig. 4. Visual comparisons for different filtering approaches for DoD_{23-15} in the upper row, and DoD_{23-18} in the lower row. Contains information © CNES (2015, 2018, 2023), Distribution Airbus DS, all rights reserved. Commercial use prohibited.

Visual inspection of figure 4 shows elevation difference trends in DoD_{23-15}, particularly the negative changes along the south part of the study area and positive changes in the north part. For DoD_{23-18}, the elevation difference is alternating between positive and negative changes. Both spatial filtering approaches, sum of sinusoid fit or spline fit, presented in figure 4 did not completely remove the along-track undulations, as found for instance by Berthier et al. [3].

Conversely, the proposed approach yields better results by significantly removing the along-track undulations while preserving the integrity of the elevation differences. Table 2 shows the evaluation metrics of the compared methods. The standard deviation and NMAD values are lower than those found in Berthier et al. [3].

Table 2. The parameters of the compared approaches.

		DoD	Sum of sine approach	Spline approach	Proposed approach
2023-2015	Mean	0.16	~ 0	~ 0	~ 0
	Std	1.78	1.63	1.62	**1.40**
	NMAD	1.32	1.05	1.04	**0.86**
2023-2018	Mean	-0.10	~ 0	~ 0	~ 0
	Std	1.21	1.10	1.09	**1.02**
	NMAD	0.92	0.78	0.75	**0.65**

Using the proposed approach, the histograms of both filtered DoDs revealed a smaller deviation compared to the respective histograms of the raw DoDs. More, in the histograms of the filtered DoDs, the mode tended mostly to zero (Fig. 5), indicating that our approach not only improves the mean value and the deviation but also the distribution itself. The mean value of DoD_{23-15}, is 0.16 m and the standard deviation is about 1.78 m. After filtering, the mean value is near zero and the standard deviation is 1.40 m. For DoD_{23-18}, the mean value is -0.10 m and the standard deviation of about 1.21 m. However, the filtered DoD_{23-18} shows a mean value is near zero and a standard deviation is 1.02 m.

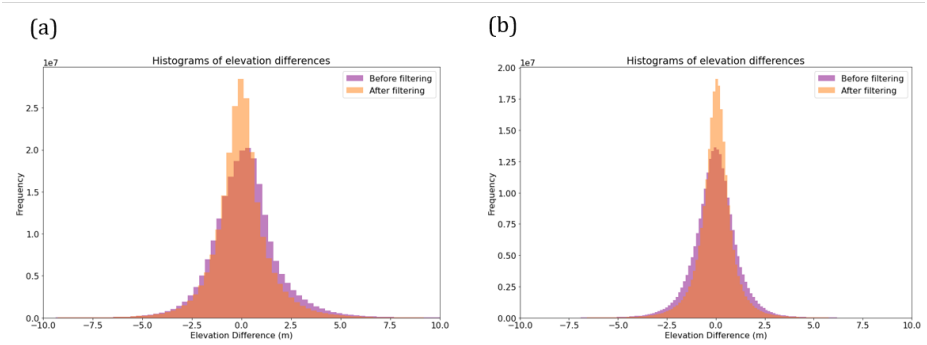

Fig. 5. Histograms of DoD_{23-15} and DoD_{23-18} before and after filtering with the proposed approach.

The slight decrease in standard deviation observed after filtering for both DoDs, can be attributed to the nature of the jitter effect, which consists of low-frequency components. These low-frequency components were attenuated through filtering process. However, the remaining variability in the data is mainly due to the changes present in the DoDs. The filtering process minimized the impact of the jitter effect noise while preserving the change features, which are relevant information for accurate 3D change detection analysis.

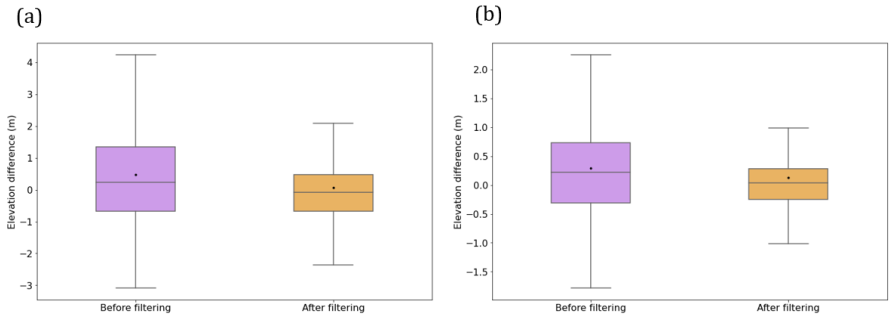

Fig. 6. Elevation difference of (a) DoD_{23-15} and (b) DoD_{23-18} before and after filtering with the proposed approach, computed on hundered of stable points. The horizontal lines within the boxes represent the median values, and the black dots represent the mean values.

Figure 6(a) shows the elevation difference in the DoD_{23-15} computed on a hundred stable points. Before filtering, the median is 0.23 m, while the median of the filtered DoD_{23-15} is -0.08 m, indicating a slightly lower central tendency for the filtered DoD_{23-15}. The spread of the data, as represented by the interquartile range (IQR), is 2.03 m for the DoD_{23-15} and 1.14 m for the filtered DoD_{23-15}, suggesting less variability.

Over the stable points, the median of the elevation difference in the DoD_{23-18} is 0.23 m, while the median for the filtered DoD_{23-18} is 0.04 m, indicating a slightly lower central tendency for the filtered DoD_{23-18}. The IQR is 1.04 m for the DoD_{23-18} and 0.54 m for the filtered DoD_{23-18}, demonstrating lower variability (Fig. 6(b)).

4 Conclusion

Significant along-track biases are specifically found within the Pléiades DEM of difference with post-2021 Pléïades 1B images, even though not they are not noticeable in the individual DEMs. It is challenging to separate noise peaks and spectrum peaks caused by spatially localized textures or repetitive patterns. Spatial filtering, while effective in smoothing noise, does not fully eliminate the jitter effect.

The proposed filtering approach is based on frequency domain filtering, which provides a more targeted solution by addressing specific frequency components that contribute to the jitter effect. This approach not only reduces the jitter effect, but also preserves fine spatial details.

The results highlight that the Fourier transform-based filtering approach offers substantial improvements over existing spatial filtering methods, as demonstrated by both qualitative visual evaluation and quantitative performance metrics. For both DoDs, DoD_{23-15} and DoD_{23-18} the mean value approaches zero.

The marginal decrease in standard deviation can be explained by the fact that the jitter effect consists of a low-frequency component, which was effectively reduced through the filtering process. However, the remaining variability is attributed to the changes present in the DoD.

Future work aims at automatically calculating the filter parameters, which, coupled with the co-alignment co-registration approach, would enable change detection across entire blocks of Pléiades images without the need for external alignment data.

Acknowledgments. This publication was made possible through support provided by the IRD.
This work has been supported by the Programme National de Télédétection Spatiale (PNTS, grant N° PNTS-2023-05).
Data from the DINAMIS device, funded by CNES, CNRS, IGN, IRD, INRAE, and CIRAD.

Disclosure of Interests. The authors declare that there are no potential conflicts of interest that could have influenced the objectivity of this research or the writing of this paper.

References

1. Ayoub, F., Leprince, S., Binet, R., Lewis, K.W., Aharonson, O., Avouac, J.P.: Influence of camera distortions on satellite image registration and change detection applications. In: IGARSS 2008-2008 IEEE International Geoscience and Remote Sensing Symposium. vol. 2, pp. II–1072. IEEE (2008)
2. Beraud, L., Cusicanqui, D., Rabatel, A., Brun, F., Vincent, C., Six, D.: Glacier-wide seasonal and annual geodetic mass balances from Pléiades stereo images: application to the Glacier d'Argentière, French Alps. Journal of Glaciology **69**(275), 525–537 (2023)
3. Berthier, E., Lebreton, J., Fontannaz, D., Hosford, S., Belart, J.M.C., Brun, F., Andreassen, L.M., Menounos, B., Blondel, C.: The Pléiades Glacier Observatory: high-resolution digital elevation models and ortho-imagery to monitor glacier change. The Cryosphere **18**(12), 5551–5571 (2024)
4. Brini, I., Feurer, D., Tebourbi, R., Vinatier, F., Abdelfattah, R.: Evaluating the potential of the Time-SIFT approach using Pléiades satellite imagery for 3D change detection. Journal of Applied Remote Sensing **19**(2), 024501–024501 (2025)
5. Deschamps-Berger, C., Gascoin, S., Berthier, E., Deems, J., Gutmann, E., Dehecq, A., Shean, D., Dumont, M.: Snow depth mapping from stereo satellite imagery in mountainous terrain: evaluation using airborne laser-scanning data. The Cryosphere **14**(9), 2925–2940 (2020)
6. Feurer, D., Vinatier, F.: Joining multi-epoch archival aerial images in a single SfM block allows 3-D change detection with almost exclusively image information. ISPRS journal of photogrammetry and remote sensing **146**, 495–506 (2018)

7. Girod, L., Nuth, C., Kääb, A., McNabb, R., Galland, O.: MMASTER: improved ASTER DEMs for elevation change monitoring. Remote Sensing **9**(7), 704 (2017)
8. Nuth, C., Kääb, A.: Co-registration and bias corrections of satellite elevation data sets for quantifying glacier thickness change. The Cryosphere **5**(1), 271–290 (2011)
9. Shean, D.E., Alexandrov, O., Moratto, Z.M., Smith, B.E., Joughin, I.R., Porter, C., Morin, P.: An automated, open-source pipeline for mass production of digital elevation models (DEMs) from very-high-resolution commercial stereo satellite imagery. ISPRS Journal of Photogrammetry and Remote Sensing **116**, 101–117 (2016)
10. Teshima, Y., Iwasaki, A.: Correction of attitude fluctuation of Terra spacecraft using ASTER/SWIR imagery with parallax observation. IEEE transactions on geoscience and remote sensing **46**(1), 222–227 (2008)
11. Wang, M., Zhu, Y., Jin, S., Pan, J., Zhu, Q.: Correction of ZY-3 image distortion caused by satellite jitter via virtual steady reimaging using attitude data. ISPRS Journal of Photogrammetry and Remote Sensing **119**, 108–123 (2016)
12. Ye, G., Pan, J., Zhu, Y., Jin, S.: A jitter detection method based on the integration imaging model. ISPRS Annals of the Photogrammetry, Remote Sensing and Spatial Information Sciences **3**, 709–715 (2020)